Mausam, (1987), 38, 2, 147-156

551.515.1 : 515.511 : 551.553.21

Further analysis on the thermal response of the upper Bay of Bengal to the forcing of pre-monsoon cyclonic storm and summer monsoonal onset during MONEX-79

R. R. RAO

Naval Physical & Oceanographic Laboratory, Cochin

(*Received 7 August 1984*)

सार — मानेक्स-79 के दौरान एकत्रित आंकड़ों की सहायता से, ऊपरी महासागरीय जल का बंगाल की खाड़ी में श्री लंका से परे स्थिर स्थिति 7.5° उ.अ. एवं 87.5° पू. दे. पर मानसून के प्रारंभ के और मानसून पूर्व के एक प्रचंड चक्रवाती तूफान की शक्ति के प्रति ऊष्मीय प्रतिक्रिया को रिकार्ड किया गया है। यह देखा गया है कि चक्रवाती तूफान का दुर्बल मानसून की शुरूआत के मुकाबले में अधिक प्रबल प्रभाव था। मिश्रित स्तरों के नीचे गर्मी का पुनर्वितरण करने में उर्ध्वाधर अभिवाही प्रक्रियाओं के महत्व को बताया गया है। तूफान के दिन, सतही स्तरों में ऊष्मीय उत्क्रमण (इनवरशन) की उपस्थिति तूफानी हवाओं के कारण उत्पन्न एकमैन अभिसरण की प्रतिक्रिया स्वरूप अपेक्षाकृत गर्म सतही जल के अवतरण के कारण है। 100 मी. से नीचे तापमान आंकड़ों के फूरियर विश्लेषण से इस बात का पता चला है कि अर्धदैनिक ज्वार-भाटे से ऊर्जा का रिसाव, तूफान वाले दिन (5 मई) से तूफान से बाद के दिन (14 मई) तक अल्पकालीन आंतरिक लहरों तक होता है।

ABSTRACT. The thermal response of the upper oceanic waters at the stationary position 7.5° N & 87.5° E off Sri Lanka in the Bay of Bengal to the forcings of a severe pre-monsoon cyclonic storm and of monsoonal onset is documented with the aid of the data sets collected during MONEX-79. It is found that the cyclonic storm had a stronger influence compared to that of weak monsoonal onset. Below mixed layer, the importance of vertical advective processes in redistributing the heat is highlighted. The presence of a thermal inversion in the surface layers on the storm day is attributed to the descent of warmer surface waters in response to the Ekman convergence caused by the storm winds. Fourier analysis of temperature data below 100 m revealed the leakage of energy from semi-diurnal tide to short period internal waves from the storm day (5 May) to a post-storm day (14 May).

1. Introduction

The energy transfer from storms is sufficiently large to produce oceanic perturbations of significant amplitude. Surface cooling and the deepening of the mixed layer in the wake of severe tropical cyclones has been reported for different oceanic areas by several workers. The response characteristics of the ocean mixed layer have been found to depend on the size, translation speed, wind strength at the eyewall etc of the storm. Several workers have offered a variety of hypotheses to explain the observed upper oceanic changes. Francis and Stommel (1955) described how gale winds of 37 knots for one day increased the depth of homogenous water from initial values of 10-30 m to depths of 6 m. Jordan (1964) reasoned that for typical mixed layer depths, large temperature variations could not be due to the heat loss to the atmosphere but must originate from the thermocline layers through vertical fluxes. Leipper's (1967) comparison of bathy thermographs (BT) before and after a storm showed outward transport of surface water, upwelling in the centre of the storm and cooling and mixing of the outward flowing water. The aerial survey with airborne expendable bathy thermographs in combination with conventional data revealed the presence of alternating cooler and warmer pools with radius in the upper layers while the subsurface data tend to show only a single upwelling cell (Black and Mallinger 1972). Fedrov's (1973) analysis on the temperature changes due to the passage of fourteen storms showed a predominant type of temperature difference profile of strong cooling (by 1°-3°C) in the upper 30 m, a warmer (0.5°-2.0°C) layer between 30 m and 90 m and a cooler layer from 90 m to perhaps 175 m. Fedrov proposed a two-cell vertical circulation in the plane perpendicular to the track of the storm. The inner cell with upwelling at the centre and downwelling at about 200 km is consistent with the observations of Leipper. Consequently, the mixed layer depth decreases near the centre and increases at larger radii. The existence of the intermediate warm layer is attributed to convective mixing due to penetrative deepening of the mixed layer. Anthes (1982) summarised the mechanisms, responsible for the lowered surface temperature as, (*i*) upwelling of cooler water, (*ii*) wind induced vertical mixing of deep cooler water with the

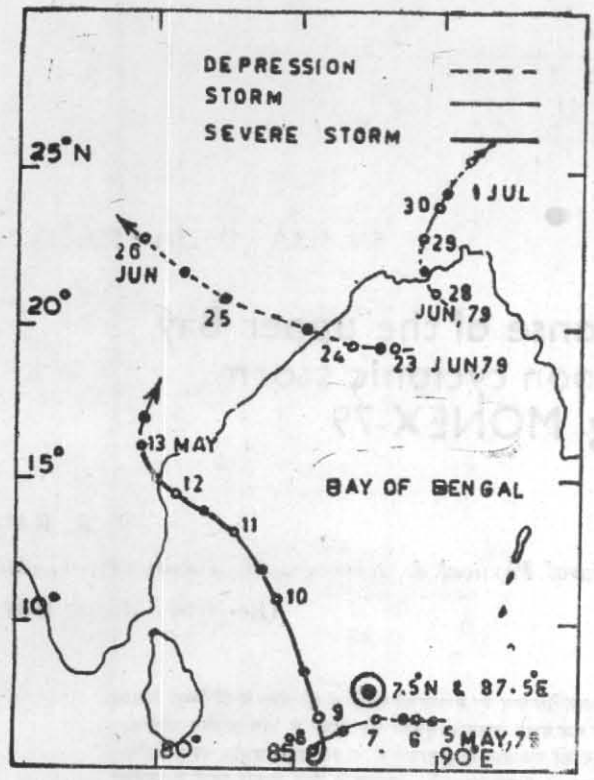

Fig. 1. Station location map and tracks of the pre-monsoon cyclonic storm and of monsoon depressions

surface waters, (*iii*) horizontal advection of cooler water by the ocean currents driven by the storm and (*iv*) loss of heat to the atmosphere. Because the effects of these processes are intermingled, the routine observations cannot completely resolve the magnitude of the contribution of each of these processes.

The information on the resulting thermal changes in the upper layers of the Bay of Bengal on account of several pre and post-monsoon cyclones is meagre due to scarcity of coincident before-after BT soundings at the same location. The monsoon experiment (MONEX-79) as a regional component of First Global GARP* Experiment carried over the Bay of Bengal provided an unique opportunity to observe the changes in the top 200 m water column at the selected station (7.5°N & 87.5°E) under the influence of a severe pre-monsoon cyclonic storm. A preliminary analysis with these data sets was reported by Rao *et al.* (1983). In the present exercise further analysis is made on the observed changes in the thermal features of the upper layers to the forcing of a pre-monsoon storm and that of summer monsoonal onset.

2. Data

One Indian ship occupied the stationary position (7.5°N & 87.5°E) east off Sri Lanka during the periods 5 to 20 May 1979 and 23 to 30 June 1979 in accordance with the observational schedule of MONEX-79. A cyclonic storm formed and strengthened in the vicinity of the stationary position and moved towards the south east coast of India during the former period (Fig. 1). Monsoon set in at the observing station around 10/11 June 1979. The later period of observation approximately corresponds to post-monsoonal onset. Time series measurements of routine marine meteorological data inclusive of global radiation and BT soundings at 1/2 hourly to 3 hourly interval were made during these periods. However, no data could be collected at the station during 6 to 13 May due to rough weather conditions associated with the strengthening cyclonic storm. But the data collected on 5 May and during 14-20 May provide very useful information on the observed changes in the subsurface thermal structure under the influence of the severe pre-monsoon cyclonic storm. A brief weather summary from Mukherjee *et al.* (1981) is given below for the storm and disturbances after the weak onset of the monsoon.

Severe cyclonic storm of 5-13 *May* 1979

A low is concentrated into a depression on the evening of 5 May with its centre near 7°N and 90°E over the southeast Bay. Moving slowly westwards and intensifying at the same time, the depression attained storm intensity by the morning of 7th near 7°N and 88°E. The storm took a westsouthwesterly track upto 8th morning while attaining hurricane intensity. After 8th, the storm took a northnorthwesterly course upto the 11th morning and later moved northwest towards south Andhra coast attaining its peak intensity on 11 and 12 May. It crossed the coast about 50 km south of Ongole by the evening of 12th and gradually dissipated by 14th morning. The temporal sequence of cloud mosaics observed in the visible band from polar orbiting ESSA satellites for the period 1-13 May 1979 is shown in Fig. 2.

Deep depression of 23-26 *June*

A low pressure area over north Bay concentrated into a depression on the morning of 23 June with its centre near 19. 5°N and 88.5°E. The depression became deep on 24th and moving westnorthwestwards across Orissa it weakened into a low by the evening of 26 June (Fig. 1).

Deep depression of 27 *June*-1 *July* 1979

A depression formed on 28 June with its centre near 21.5°N and 90°E. Moving in a northerly direction, it became deep the next day over Bangla Desh. Moving northnortheasterly direction this weakened into a depression by evening of 1 July (Fig. 1).

3. Analysis and discussion

The distribution of daily totals of observed net available insolation after applying correction for albedo (Q_I), estimates of total heat losses by the ocean (Q_L), as the sum of the net long wave radiation following Reed (1976), sensible and latent heat fluxes estimated with the exchange coefficient following Kondo (1975) and the balance of net oceanic heat gain/loss (Q_N) is shown in Fig. 3. Positive values imply gain to the sea. Values corresponding to 5 May '79 are shown with a dot in a circle. Missing values for the period 6-13 May may be noted. Lowest Q_I value of 55 cal/cm²/day on 5 May is on account of overcast skies in association

*Global Atmospheric Research Programme.

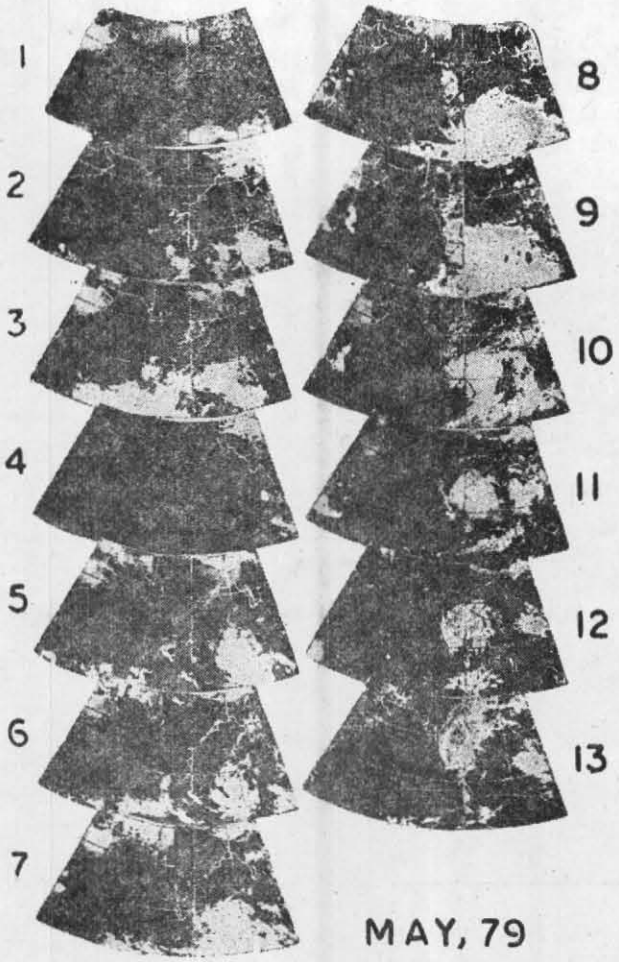

Fig. 2. Time sequence of satellite cloud pictures over the north Indian Ocean, 1-13 May 1979

with the depression. During the post-storm period Q_I fluctuated around 500 cal/cm²/day due to clear skies. After the onset of the monsoon Q_I is also of similar magnitude with the exception on the initial two day period (*i.e.*, 23-24 June) owing to the formation of a monsoon depression over the head Bay. The total heat fluxes to the atmosphere are high on 5 May and 23 June with an approximate values of — 400 cal/cm²/day and — 500 cal/cm²/day respectively. Heat losses (Q_L) gradually built up during the post-storm period from 16 May due to the strengthening southwesterlies over the south Bay. During the post-onset phase the average value of Q_L is — 370 cal/cm²/day. Net oceanic heat gain (Q_N) is mostly positive indicating a gain to the sea with the exception on 5 May and 23 June. Q_N varied between 300 cal/cm²/day and 400 cal/cm²/day during the post-storm period. During the post-onset phase Q_N varied between — 200 cal/cm²/day and 200 cal/cm²/day.

The distribution of daily averaged sea surface temperature (SST), mixed layer depth (MLD) and vertical gradient in the upper thermocline is depicted in Fig 4. MLD is defined as the depth where the below layer gradient of 1.0°C/10 m persisted in a 30 m water column. The averaged bulk vertical thermal gradient (°C/10 m) in the topmost 200 m water column below mixed layer is shown in the lower panel. The surface cooling of over 3°C is quite evident from 5 to 14 May. The retreat is also significant of the order 2°C/week. If cooling of 3°C of the 45 m layer (average of pre-and post-storm mixed layer depths) occurred only through surface heat fluxes the losses should be of the order of —1500 cal/cm²/day. Even though such high fluxes are not ruled out during severe storms (Black and Mallinger 1972 reported an average oceanic loss of —1000 cal/cm²/day) the resulting post-storm BT profile should reflect a well developed isothermal layer due to consequential convective mixing. In this case no such pattern is noticed

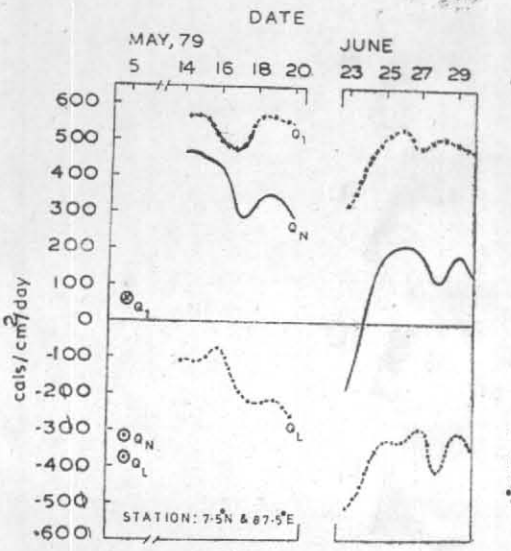

Fig. 3. Daily march of heat budget components

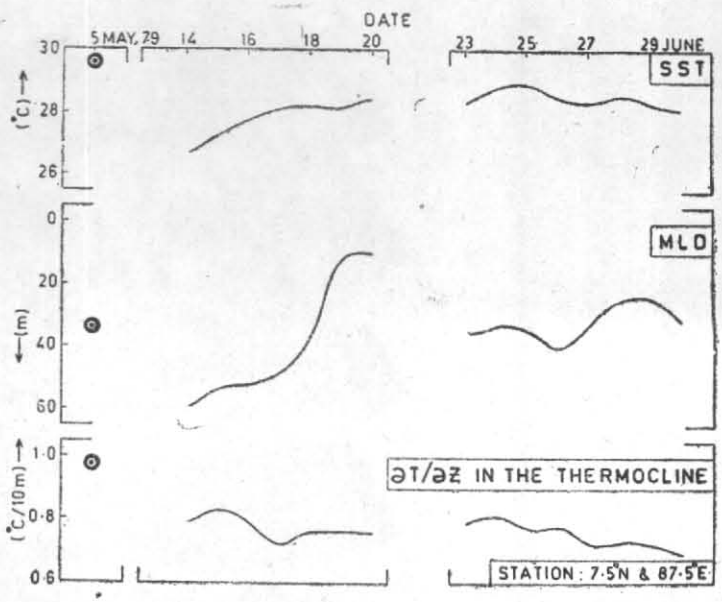

Fig. 4. Daily march of SST, MLD and below layer thermal gradient

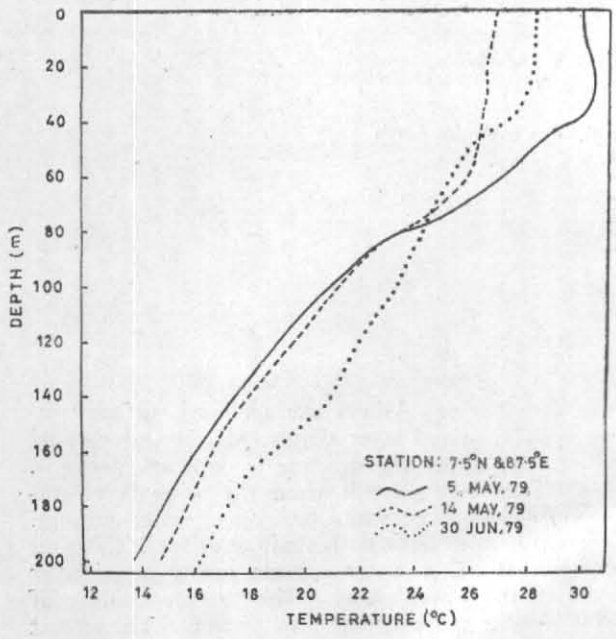

Fig. 5. Typical BT profiles for selected days

from Fig. 5. It may imply that the contributions from other processes are also important in lowering the mixed layer temperature. The mixed layer depth nearly doubled from 30 m on 5 May to 60 m on 14 May followed by a very rapid shoaling of the order of 50 m/week (Fig. 6). Even the retreat in the layer depth during post-storm period cannot also be explained in terms of surface heat exchanges alone. The upwelling below mixed layer (Fig. 7) might have contributed to the significant shoaling of the mixed layer. The layer depth varied between 30 m and 40 m during the post-onset phase. The progressive reduction of the vertical thermal gradient below mixed layer after both the events probably resulted due to the divergence of the isotherms (Fig. 7).

Typical daily averaged BT profiles of the top 200 m water column are shown in Fig. 5 depicting the conditions during pre-storm (5 May), post-storm (14 May) and post -onset (30 June). The profile of 5 May shows a mild positive gradient between 10 m and 30 m in the surface layers. Significant cooling is seen in the topmost 80 m water column from 5 to 14 May. No prominent changes are perceptible below 80 m indicating that storm impact is confined to only topmost 80 m layer or so. On the other hand, after the monsoonal onset, downwelling (from 14 May to 30 June) of the order of 0.5 m/day is conspicuously seen through the upper thermocline. The large scale negative wind stress curl (Wylie and Hinton 1982) might have induced the observed downwelling. Well mixed isothermal layer in the top is obvious in the profile of 30 June because of wind and buoyancy mixing. The heat content of the topmost 80 m layer is lowered by 18.3 K cal/cm² from 5 to 14 May.

The temporal evolution of daily averaged BT profiles for the pre- and post-storm regimes is shown in Fig. 6. Hatched areas show waters warmer than 25°C. The reduction in the heat content with respect to 25°C is

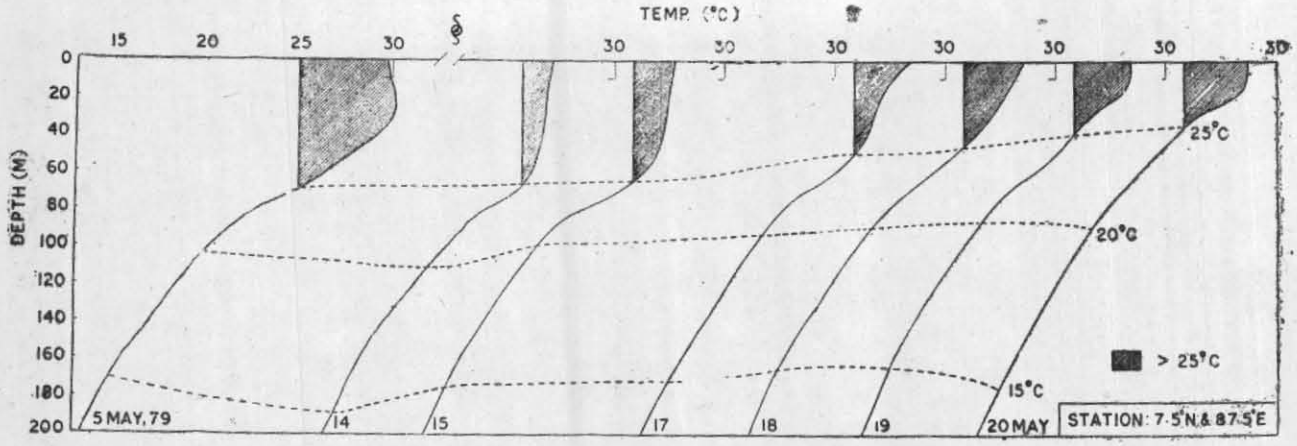

Fig. 6. Time sequence of BT profiles corresponding to storm event

distinctly seen during 5 to 14 May. During the post-storm period the values slowly increased. This is in accordance with the accumulation of heat through Q_N. In the upper thermocline 25°C isotherm ascended by 30 m from 14 to 20 May implying an upwelling rate approximately of 5 m/day. Relatively weaker ascent is noticed for 20°C and 15°C isotherms.

The depth-time section of thermal field from 5 May to 30 June, with intermittent discontinuities is shown in Fig. 7. The daily averages of BT data of the top 200 m water column are contoured at 1°C interval. On 5 May a subsurface warm slab extending approximately from 15 m to 35 m with temperature greater than 30°C is seen. With the intensification and passage of the storm, these features are no longer seen on 14 May. Instead a relatively colder and deeper mixed layer is found. In the following one week from 14 May through SST increased by 1.7°C the mean temperature of the top-most 30 m water column increased by 1°C. This 1°C rise is possible with a net oceanic heat gain of 430 cal/cm²/day over a seven day period. With the assumption that the solar radiation penetrating below 30 m depth is negligible the estimated net oceanic heat gain (Q_N) of 370 cal/cm²/day for this period (Fig. 3) is almost in balance. Indirect inaccurate estimates of insolation values for this period by Rao *et al.* (1983) led them to offer advection of heat responsible for this rise of temperature. Solar heating during the intervening period from 20 May to 23 June might have resulted an increase of 1°C in the mean temperature of the 30 m water column. With the progress of the monsoon a corresponding cooling of 0.5°C occurred in the last week of June. In the upper thermocline very conspicuous changes in the nature of isotherms slopes are noticed.

During the storm period from 5 to 14 May, the isotherms above 80 m depth ascended while there is descent below. *Similar phenomenon is also* noticed around 100 m depth during the period of post-onset (20-30 June). The cyclonic wind stress pattern causes the Ekman or mixed layer transport to be divergent. This divergence will be balanced by upwelling at the base of the mixed layer and by lateral convergence below. The ascent of isotherms in the upper 80 m to 100 m might have governed by direct wind stress curl while below these depths the descent of isotherms might have resulted due to baroclinic adjustments (Kraus 1972). During the post-storm period (14-20 May) all the isotherms have shown upward slopes with an average ascending rate of 4 m/day. The slopes weakened with depth. This strong retreat might be viewed as a segment of the inertial oscillation set in the wake of this severe storm (Pollard 1972). During the period 20 May-23 June all the isotherms descended of the order of 1 m/day due to the negative wind stress curl (Wylie & Hinton 1982). During the post-onset period, the upward slopes of the isotherms in the top 100 m water column is evident in consequence to the wind stress curl associated with the monsoonal flow.

The pattern of heating/cooling regimes with respect to 5 May in the top 200 m water column is shown in Fig. 8. Positive values indicate cooling with respect to 5 May. Hatched areas indicate cooling greater than 2°C. The magnitude and vertical extent of cooling is higher in the case of the storm compared to that of the monsoonal onset. The cooling in the upper layers resulted due to the combined effect of mixed layer cooling and upwelling below. In the top 20 m layer the cooling progressively diminished from 14 to 20 May due to solar heating. During the same period, below 40 m the cooling pattern descended on account of ascent of colder waters. During the period of post-onset a warming of 2 to 3°C is noticed below 70 m mostly on account of sinking.

Cyclone heat potential (CHP) and heat content (HC) of the topmost 10 m, 100 m and 200 m layers are computed following Rao *et al.* (1983) and the distributions are shown in Fig. 10. The reference temperature of 28°C is chosen in estimating the CHP as most of the cyclones in tropics from when SST $\geq$ 28°C. A drop of 8 K cal/cm² is noticed from 5 to 14 May implying a net oceanic heat loss of atleast —900 cal/cm²/day (The possibility of

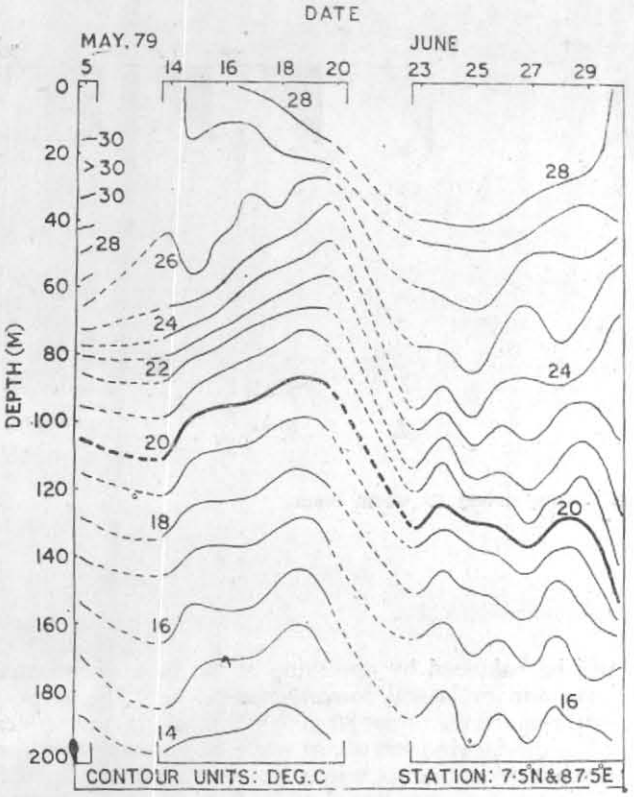

Fig. 7. Depth-time section of temperature of topmost 200 m layer

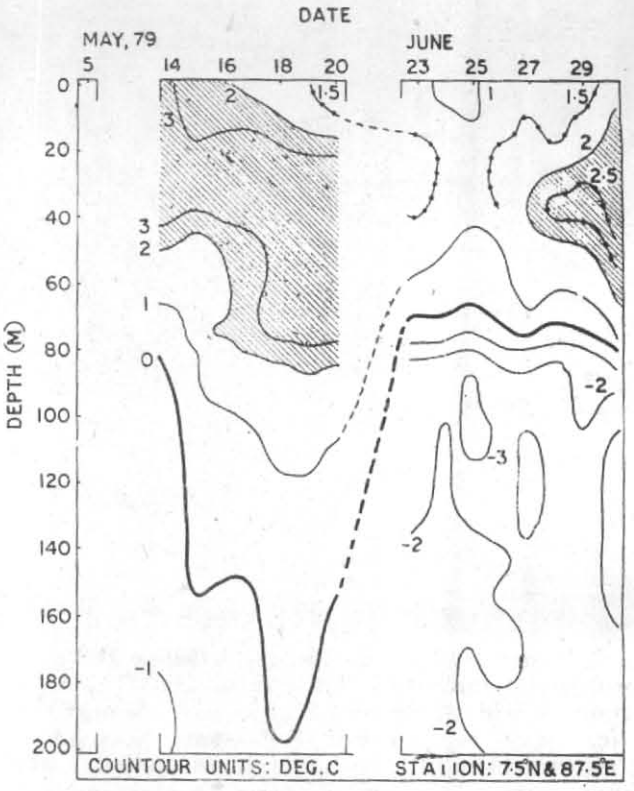

Fig. 8. Depth-time section of heating/cooling regimes with respect to 5 May in the topmost 200 m layer

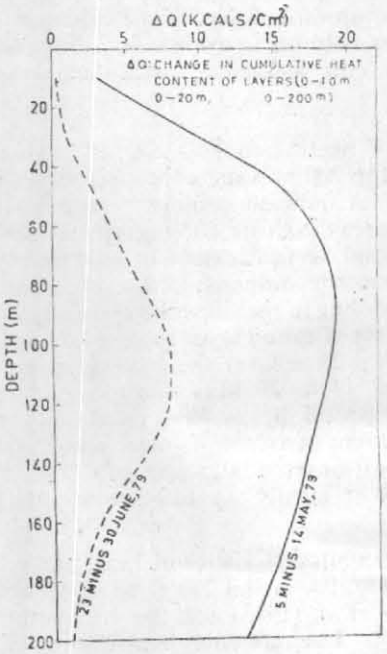

Fig. 9. Temporal change in the cumulative heat content of upper layers for the storm and monsoonal post-onset events

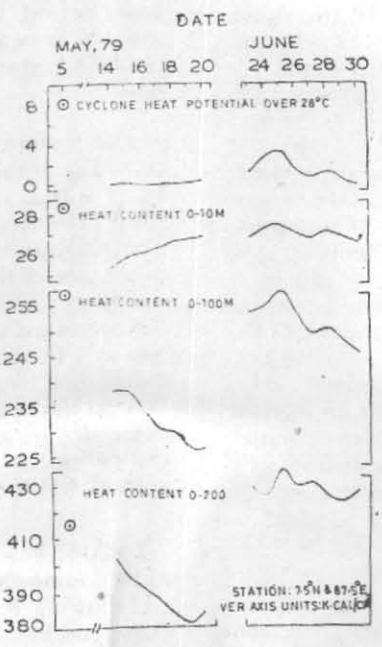

Fig. 10. Daily march of cyclone heat potential, heat content of topmost 10 m, 100 m and 200 m layers

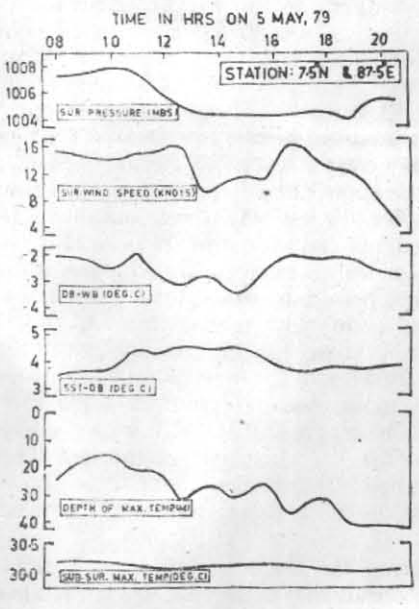

Fig. 11. Hourly march of surface marine meteorological parameters on 5 May

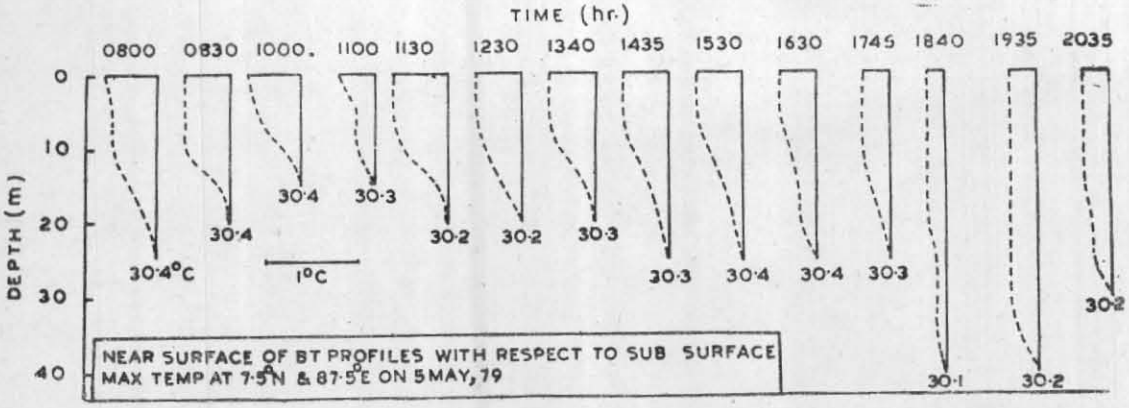

Fig. 12. Hourly march of BT profiles showing positive gradient below surface on 5 May

the occurrence of zero K cal/cm² before 14 May cannot be ruled out which may even imply a higher net surface heat loss during the storm weather). Above argument is valid if other processes as advection and entrainment are not important. During the post-onset phase the CHP registered a gradual fall. Significant fall is noticed in the HC of all the three layers from 5 to 14 May. During the post-storm regime only the HC of top 10 m layer showed a retreat due to intense solar heating while those of top 100 m and 200 m layers further decreased due to upwelling of colder waters from below. During the intervening period of one month from 20 May, the HC values again shot up due to sinking of relatively warmer waters from above. During the post-onset phase the HC values registered a fall for all the three layers. However, the corresponding fall is highest for top 100 m layer due to the observed upwelling above 100 m. The trend for top 200 m layer is not conspicuous due to combined processes of upwelling above 100 m bepth and sinking below. On the whole, the changes brought out in the HC values are mostly governed by vertical advective processes controlled by Ekman and probably geostrophic transports.

The temporal changes occurred in the cumulative heat content of topmost 0-10 m, 0-20 m, 0-30 m, .., and 0-200 m slabs for both the events is shown in Fig 9. The pattern of both the curves is similar with differences in the magnitudes and the depths of occurrence of maxima. Storm forcing is shown to be much stronger especially in the surface layers compared to that of monsoonal onset. Highest change of 19 K cal/cm² occurred in the top 90 layer for the storm event while the corresponding value is 8 K cal/cm in the top 120 m layer for the monsoonal flow. Though the impact is stronger in the storm event, the downward penetration of the forcing is greater in the later probably due to the differences in the respective spatial extents.

Marine meteorological data collected at slightly irregular intervals (half hour to one half hour) on 5 May are shown in Fig. 11. These data reflect the near surface atmospheric characteristics when the pre-monsoon cyclonic storm is strengthening. A drop of nearly 4 mb within four hours from 1000 hrs (LST) is clearly noticed. *This pressure drop could be* due to both diurnal oscillation and storm intensification. Winds fluctuated around 12 knots. The negative wet bulb depression throughout indicates super saturation conditions near the surface. The drop of 1°C roughly coincided with the period of pressure drop (1000 to 1400 hrs) is mostly due to the reduction of dry bulb temperature. A similar pattern in SST *minus* dry bulb temperature is also evident but with a reversed nature. The depth of subsurface maximum temperature progressively deepened from nearly 20 m to 40 m during this 12-hour period implying a descent rate of approximately 2 m/hr, probably caused by Ekman type of transports leading to convergence in the surface layers. No prominent changes in the subsurface maximum temperature are reflected probably indicating the non-penetration of surface mixing processes to these depths. The vertical BT profiles with respect to the subsurface maxima in the near surface waters on 5 May are shown in Fig. 12. A thermal inversion prevailing in the depth range of 10-30 m water column is noticed throughout. The resulting instability will be discussed with the aid of Fig. 13. The subsurface maxima prevailed throughout from 0800 to 2035 hrs. The BT profiles are mostly rounded in nature reflect sinking associated with the storm driven advection. The surface waters of 30.4°C might have descended under the influence of the storm. The vertical gradients are steeper in the lower portion of the inversion layer compared to the upper. This may imply that mixing might has been initiated to homogenise the top strata of the water column under the influence of wind and wave action. With the progress of time, this can be further inferred from the facts that (*i*) the temperature difference of SST and subsurface maxima gradually diminished & (*ii*) the length of isothermal layer progressively increased. This clearly reveals that the mixing time scales of the upper layers of the ocean to the storm forcing are of the order of few hours (Francis and Stommel 1955). The stability $E\left(\frac{1}{\rho}\ \frac{\partial \rho}{\partial z}\right)$ of the near surface inversion layer is calculated with temperature and salinity data at the surface and the depth of subsurface maximum temperature and is shown in Fig. 11. Values of E are negative throughout indicating unstable stratification in the inversion layer due to lower density of the water at the base of the inversion layer. Highest instability prevailed around 1000 hours followed by progressive fall due to mixing caused by wind and buoyancy fluxes. The rapidity in the fall of E is marked from 1000 hrs. Near neutral equilibrium conditions are attained rapidly in the following 10 hours

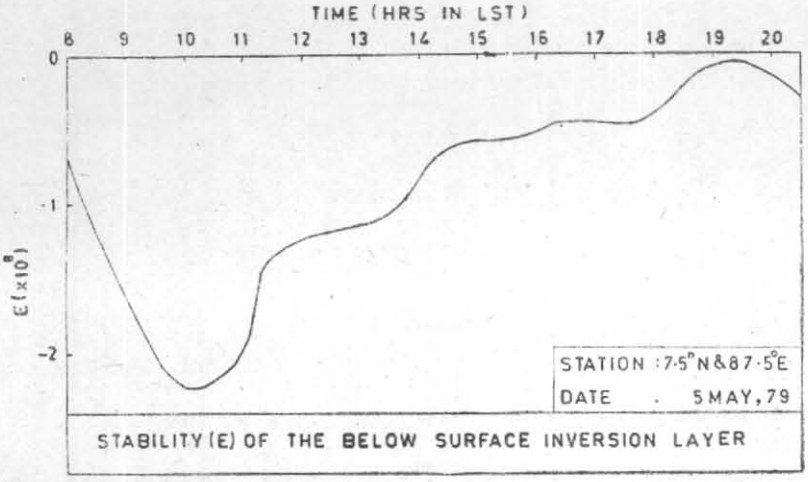

Fig. 13. Hourly march of static stability of the near surface thermal inversion layer on 5 May

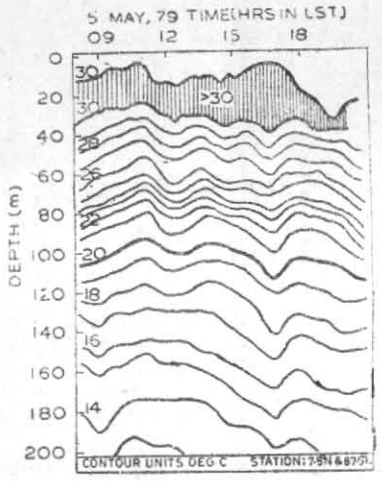

Fig. 14. Depth-time section of temperature of the topmost 200 m layer on 5 May

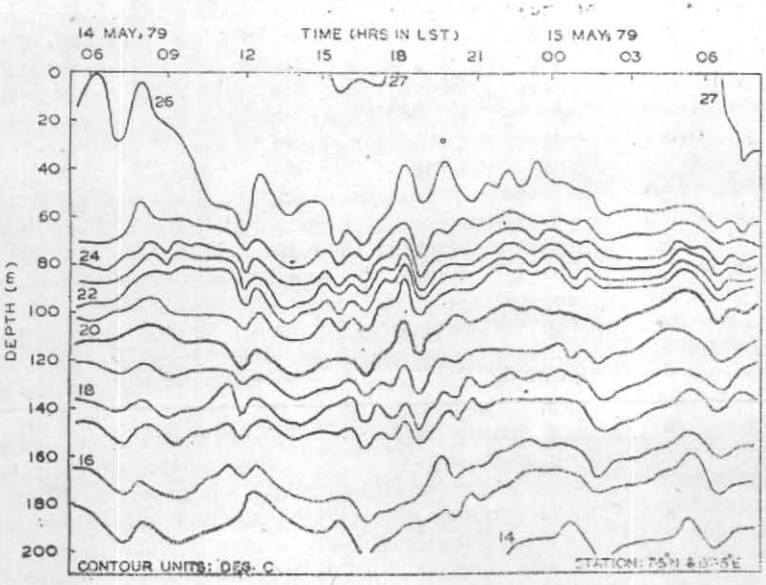

Fig. 15. Depth-time section of temperature of the topmost 200 m layer on 14/15 May

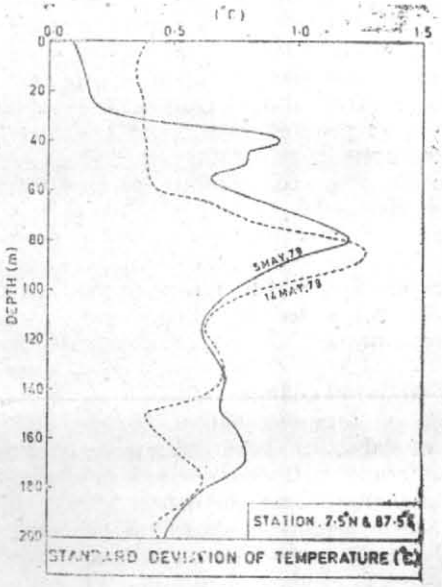

Fig. 16. Standard deviation of temperature in the topmost 200 m layer on 5 and 14/15 May

Depth-time field of temperature for the 13-hour period on 5 May is shown in Fig 14. Isotherms are drawn at 1°C interval with a few interpolations in the temporal domain. The subsurface warm layer (>30°C) is shaded for better perception. Deepening tendency of this warmer layer can be noticed. Descent of isotherms below the mixed layer probably under the influence of internal tide is also evident. The vertical thermal gradient between 40 m and 100 m is double (1.5°C/10 m) that of the gradient of the layer between 100 m and 200 m depths (0.7°C/10 m). Similar strong gradients are also observed in the halocline above 100 m depth. Embedded wavy nature of isotherms is seen throughout with some differences in depth. Above 100 m depth approximately four peaks are seen while the number of peaks diminished with depth. This shows higher perturbation frequency in the stronger stratified layer above 100 m depth under the storm forcing from above. In addition, the average wave amplitude increased with depth. The corresponding depth-time field of temperature on 14/15 May is shown in Fig. 15. In the well developed near surface mixed layer, day time heating is manifested with the

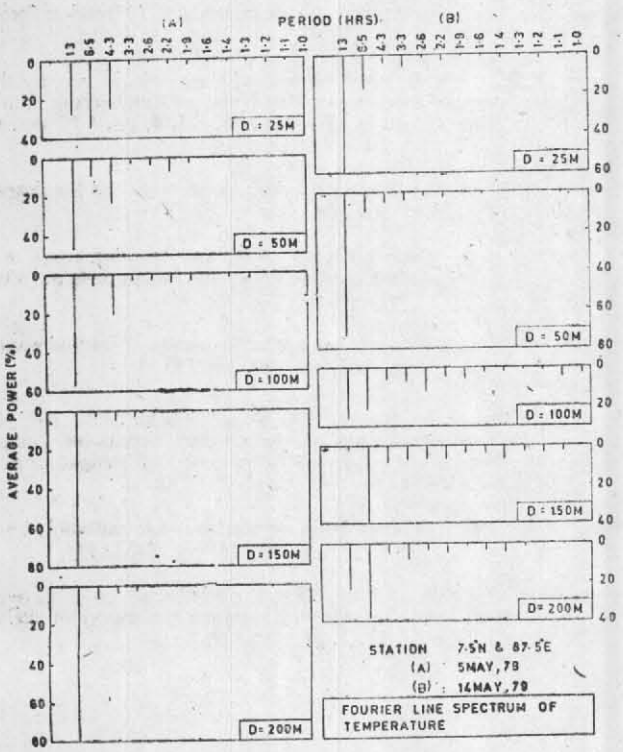

Fig. 17. Fourier line spectra of temperature at selected depths on 5 and 14/15 May

transitory appearance of 27°C isotherm. On the whole increased wave number is noticed throughout compared to that of 5 May.

The standard deviation of temperature with depth for these two days is shown in Fig. 16. On 5 May two distinct modes are noticed around 40 m and 80 m depths where vertical thermal gradients are also high leading to enhanced internal wave activity. With the passage of the storm, *i.e.*, on 14th the upper mode of 5th disappeared with the deepending of the mixed layer while the lower one slightly descended. At this depth ($\sim$ 85 m), the isotherms have shown opposite slopes (ascent above 80 m and descent below 80 m) from 5 to 14 May (Fig. 7).

Following Jenkins & Watts (1968), Fourier analysis of time series of mean removed temperature data of 5 and 14 May 1979 has been made at selected depths 25,50,100, 150 and 200 m. The corresponding line spectra are shown in Fig. 17. The average power is depicted in percentage for easier comparison. The fundamental frequency (13-hr period) corresponding to semi-diurnal internal tide is quite prominent at all the depths on 5 May, while on 14 May this feature persisted only upto 100 m depth. Below 100 m depth there is a shift in the maxima to the first harmonic (6.5-hour period) corresponding to quarterdiurnal tide. This first harmonic is also stronger at 25 m depth on 5 May. The second harmonic (4.3-hr period) is relatively stronger on 5 May compared to 14 May in top 100 m layer. This may imply that an internal wave of this period is prominently developed only under the influence of storm on 5 May. With the passage of storm this 4.3-hour wave might dampened out by 14 May. Further, relatively higher spectral power is found with the higher sub-harmonics below 100 m depth on 14 May compared to those of 5 May. Larsen (1969) reported an interesting case of possible generation of short period internal waves by a storm.

4. Summary and conclusions

(*i*) Cooling and deepening of the mixed layer is more prominent during the storm event compared to that of the weak post-onset regime of the monsoon. The cooling is of the order of 3°C and 1°C respectively. The deepening is 30 m in the former event. The retreat during the post-storm period is of the order of 2°C and 50 m per week. Data are inadequate to resolve the contributions of various processes responsible for the observed changes.

(*ii*) Distinct upward/downward tendencies are noticed in the depth-time field of temperature as a consequence of vergence due to Ekman and probable geographic transports. These resulted strong thermal changes of 2° to 3°C in the temporal domain.

(*iii*) Temporal changes in the bulk integral of heat content of the upper layers is larger for the storm event (19 K cal/cm^2 in the top 90 m layer) compared to that of post-onset (8 K cal/cm^2 in the top 120 m layer). This implies that stronger redistribution of heat to have taken place in the vertical during the storm event.

(*iv*) During the storm day a thermal inversion is present approximately embedded between 10 m and 30 m depths. Subsurface maximum temperature of 30.4°C is present due to the descent of surface warm waters caused by Ekman type of convergence.

(*v*) Analysis of temperature in the high frequency domain revealed the presence of internal waves. Leakage of energy from semi-diurnal internal tide to the short period waves is noticed below 100 m from the storm day (5 May) to the post-storm day (14 May).

Acknowledgements

The author wishes to thank Dr. D. Srinivasan for his keen interest and for providing facilities to carry out this investigation. The author is grateful to some of his colleagues who collected and processed BT data and to scientists from India Meteorological Department who collected and processed marine meteorological data inclusive of radiation during MONEX-79 experiment. The author is grateful to the referee for suggesting improvements.

References

Anthes, R.A., 1982, Tropical cyclones, their evolution, structure and effects, Meteorological Monographs, 19, 41, American Meteorological Society, Boston, Mass., USA, 208 pp.

Black, P.G. and Mallinger, W.D., 1972, The mutual interaction of hurricane Ginger and the upper mixed layer of the ocean, 1971, Project Stormfury Annual Report, Dept. of Commerce, Washington, D.C., pp. 63-87.

Fedrov, K.N., 1973, The behaviour of the ocean surface active layer under the influence of tropical hurricanes and typhoons, *Oceanology*, **12**, 3, pp. 387-393.

Francis, J.R. and Stommel, H., 1955, How much does a gale mix the surface layer of the ocean, *Quart. J. R. Met. Soc.*, **79**, 342, pp. 534-537.

Jenkins, G.M. and Watts, D.G., 1968, *Spectral analysis and its applications*, Published by Holden-Day, 525 pp.

Jordan, C.L., 1964, On the influence of tropical cyclones on the sea surface temperature field, Proceedings of the Symposium on Tropospheric Meteorology, Newzealand Meteorological Service., Wellington, pp. 614-622.

Kondo, J., 1975, Air-sea bulk transfer coefficients is diabatic conditions, *Boundary Layer Met.*, **9**, pp. 91-112.

Kraus, E.B., 1972, *Atmosphere-Ocean Interaction*, Clarendon Press, Oxford, 268 pp.

Larsen, L.H., 1969, Internal waves and their role in mixing the upper layers of the ocean, The Trend in Engineering, Univ. of Washington, Seattle, Washington, **21**, 4, pp. 8-11 and p. 19.

Leipper, D.F., 1967, Observed ocean conditions and hurricane. 'Hilda', *J. atmos. Sci.*, **24**, 2, pp. 182-196.

Mukherjee, A.K., Ramakrishnan, A.R. and Jambunathan, R., 1981, Cyclones and depressions over the Indian Seas in 1979, *Mausam*, **32**, 2, pp. 115-126.

Pollard, R.T., 1970, On the generation by winds of inertial waves in the ocean, *Deep Sea Res.*, **17**. pp. 795-812.

Rao, R.R., Rao, D.S., Murthy, P.G.K. and Joseph, M.X., 1983, A preliminary investigation on the summer monsoonal forcing on the thermal structure of upper Bay of Bengal during MONEX-79, *Mausam*, **34**, 3, pp. 239-250.

Reed, R.K., 1976, An estimation of net longwave radiation from the oceans, *J. Geophys. Res.*, **81**, 33, pp. 5973-5794.

Wylie, D.P. and Hinton, B.B., 1982, The wind stress patterns over the Indian Ocean during the summer monsoon of 1979, *J. Phys. Oceangr.*, **12**, 1, pp. 186-199.